Journal of Electronic Materials, Vol. 9, No. 3, 1980

AUGER ANALYSIS OF THE PbS-Si HETEROJUNCTION*

H. Elabd and A. J. Steckl

Rensselaer Polytechnic Institute
Troy, New York 12181

(Received June 27, 1979; revised January 9, 1980)

The chemical structure of the solution-grown PbS-Si heterojunction was studied by Auger Electron Spectroscopy. Auger depth profiles indicate a PbS film of uniform composition. No major contaminants were observed in the bulk of the PbS film. At the PbS-Si interface the only impurity observed was an oxygen peak, corresponding to approximately 1% atomic concentration. Heating the growth solution enhances the chemical reaction and deposition rates without altering the profiles of the elements at the interface. Similar oxygen peaks were detected at the Au-PbS interface and at the interface between consecutive PbS films. The interface oxygen concentration in the PbS-Si (100) structure is roughly twice that present in the PbS-Si (111) structure. Heat treatment in air increased the interface and surface oxygen concentration by a factor of 2 to 5. The same treatment in N_2 ambient had only a slight effect on the surface oxygen concentration but enhanced the interface oxygen concentration. The oxygen at the Au-PbS interface showed similar sensitivity to heat treatment. Oxygen content at the interface of HJs formed on unpolished Si was double that in HJs formed on

---

* This paper was presented in part at the Electronic Materials Conference, June 1979, Boulder, CO.

0361-5235/80/0500-0525$03.00/1

polished Si. The relative intensity of the S to Pb peaks in the bulk of the PbS film compares closely with that measured on the cleaved surface of natural single crystal galena. The Pb:S peak ratio was roughly constant throughout the PbS film and at the PbS-Si interface. Fe and Cl contaminants were observed at the surface of the PbS film, along with significant changes in the Pb:S ratio. The simultaneous detection of Pb, S and Si near the interface is attributed to the presence of surface irregularity caused by a secondary PbS macrostructure consisting of isolated chain-like clusters.

Key words: Heterojunction, Lead Sulfide, Auger Analysis.

Introduction

Solution grown PbS-Si heterojunctions (HJ) [1,2] were found to exhibit substantial IR sensitivity [3,4,5]. A study of the chemical structure of these HJs using Auger Electron Spectroscopy (AES) was performed and is presented here. In the AES experiments the PbS and Si surfaces were excited by a primary electron beam, while the energies of the secondary electrons, emitted as a result of the Auger effect [6], were used to identify the surface constituents.

The Auger spectra of chemically deposited PbS thin films on silicon and glass substrates were recorded. Since the Auger peak heights are proportional to the concentrations of the corresponding atomic species [7], the relative intensities of the lead, Pb_{NOO}, and sulfur, S_{LMM}, Auger peaks were used to determine any change in surface composition. The S:Pb peak ratio was averaged for each film and compared to that of natural galena crystals.

The S:Pb peak ratio for chemically deposited PbS film was found to be roughly equal to that measured on the cleaved surface of natural galena for most samples. Depth-composition profiles of the PbS film and the PbS-Si interface are presented in the section on Auger profiles of heterostructures. The profiles were obtained from AES scans recorded while simultaneous argon ion sputter etching erodes the specimen surface. The spatial distribution of the constituents was determined by AES scanning of the top surface as well as at different levels in the etching process. In general, PbS films prepared by chemical deposition were found to be uniform in composition in every direction to within the accuracy of AES measurements. No major contaminants were observed in the bulk of the film. No impurity peaks, with the exception of oxygen, were detected at the interface. Depth-composition profiles of multilayer PbS films are presented and discussed in the next subsection. In the heat treatment section the effect of short term, low temperature heat treatment in air on the Au contact to the PbS film is evaluated. The effect of long term, low temperature treatment, in air and nitrogen environments, on the oxygen concetration at the PbS-Si interface is discussed in the final section.

Experimental Technique

The PbS-Si HJ is formed by room temperature solution growth of a PbS film from the reaction of thiourea, $(NH_2)_2CS$, and $Pb(NO_3)_2$ [1,2]. Constituents of the chemical solution are listed in Table I. Lead nitrate and thiourea decompose

Solution	Molar Concentration	Parts in the Solution
Lead Nitrate, $Pb(NO_3)_2$	0.175 M	1
Sodium Hydroxide^A, NaOH	0.57 M	3
Thiourea^B, $(NH_2)_2$ CS	1.00 M	1
Di-Water, H_2O		12.5

A) The Molar solution of NaOH is prepared by titration.

B) The growth solution is sulfur rich, with 5.71 times the equivalent weight of sulfur for stoichiometric PbS.

Table I Constituents of the PbS Growth Solution by the catalytic action of sodium hydroxide. The released sulfur and lead ions combine to deposit PbS. The PbS deposition is discussed in detail elseware [2]. Typical PbS film thickness was around 2000Å. Single films as thin as 900Å and multiple films as thick as 4500Å have also been fabricated.

Scanning electron microscopy (SEM) and X-Ray diffraction studies show [2] that the PbS crystallite size varies between 0.2 and 0.4 µm. A secondary PbS microstructure consisting of isolated chain-like clusters, was found to coexist with the thin film as shown on Fig. 1(a). The dimensions of the clusters varied, some were up to an order of magnitude larger than the thickness of the film. For example, clusters of 3 to 4 µm were measured on a film of 0.45 µm thickness as shown on Fig. 1(b). The microstructure and composition of the cluster were found to be similar to that of the film.

Most of the experiments were carried out with a PHI 10-234 GC Cylindrical Auger Electron Optics System. In this system, the Auger beam has a nominal diameter of 0.05 to 0.08 cm. The measurements were carried out while the samples

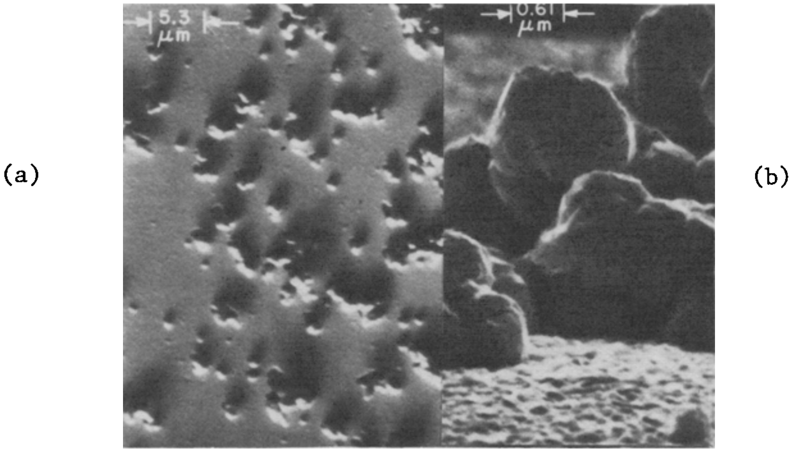

Fig. 1a, b. Secondary Electron Micrograph of a PbS film on Si(100) and PbS Cluster after Thermal Etching are nominally kept at room temperature. The working principles and the electronics of the cylindrical mirror analyzer in AES have been discussed in more detail elsewhere [8,9]. The maximum detection limit of elements is estimated to be 0.1 at.% [8,9]. In addition to the experiments performed on the PHI 10-234, two samples were tested on the PHI SAM-590 system to investigate the sample uniformity using a narrow (1μm) electron beam. Sputter etch rate calibration was carried out using SiO_2 and NiO films of known thickness [10].

The spectra of the pure elements (e.g. lead, sulfur, silicon and oxygen) were studied and documented by the manufacturer of the AES System [11]. The depth profiles of the PbS-Si HJ and natural galena* samples were evaluated by monitoring the two strongest peaks of each element (Pb, S, Si) in the structure. Table II shows a listing of the appropriate elements, relative signal contribution, atomic number, Auger transitions and corresponding energies for the elements appearing in the compound heterojunction system. In the Auger spectrum of Pb, the major peak is the 90-94 eV doublet, which can be associated with the NOO Auger transition. At the same time the major Si peak is the KLL transition at 92 eV, overlapping the Pb doublet. Since this prevents clear differentiation of the two elements at the interface, secondary Auger transitions, Si_{LMM}: 1619 eV and Pb_{NOO}: 249-267 eV, were also recorded. Carbon appeared as a trace component at the surfaces of glass and silicon.

As a point of reference Auger depth profiles of cleaved galena crystals were recorded. No impurity peaks were observed in the spectrum with the exception of a small oxygen peak at 510 eV. The relative amplitudes of the Auger peaks remained fairly constant in the bulk. The S:Pb ratio changed by ± 5% along the depth of the crystal, excluding a surface layer of 150Å. To estimate the percentage oxygen present in the bulk the amplitude of the oxygen peak was

---

* Purchased from Ward's Natural Science Establishment Inc., Rochester, N.Y.

Table II Components of the Auger Spectrum of the Heterojunction Systems

ELEMENT	APPEARANCE	ATOMIC NUMBER	AUGER TRANSITION	ELECTRON ENERGY (eV)
LEAD	Major Component in PbS Film	82	$Pb_{NOO}(N_7O_{4,5}O_{4,5})$	90-94
			Pb_{NOO}	249-267
SULFUR	Major Component in PbS Film	16	S_{LMM}	152
SILICON	Major Component in Si	14	Si_{LMM}	92
	Substrate		Si_{KLL}	1619
OXYGEN	Minor Component at the Interface (0.1-2%)	8	$O_{KLL}(K\ L_{2,3}L_{2,3})$	510
CARBON	Trace Component at the Surface (0.1 - 0.6%)	6	C_{KLL}	272
ARGON	Minor Component Embedded in Si (0.1 - 5%)	18	Ar_{KLL}	215

compared to that detected in the spectra of SiO_2. The comparison yields 3·6 at.% for oxygen concentration in the bulk.

The relative intensities of S_{LMM} (152 eV) and Pb_{NOO} (90-94 eV) for single crystal galena samples and for thin film PbS samples were computed for every Auger scan and depth averaged. This depth average is referred to as the $S:Pb_1$ ratio. The Auger scans of the first 300Å below the surface were excluded from the computation since they yield data not representative of the bulk conditions.

The average relative intensity of $<S:Pb_1>$ for galena samples was 2.9, which may be taken as a rough estimate of the intensity ratio of these two peaks under steady state conditions and for surface roughness compared to that of a cleaved galena sample. The intensity ratio $<S:Pb_1>$ for thin film PbS samples was in the range 2.8 to 3.0. In the Auger spectrum of Pb and of the PbS film several small Auger peaks appear at 60 eV and below. These peaks were not included in the plotting of subsequent depth profiles. The lead doublet at 90 to 94 eV appears merged into one peak in the Auger spectrum of galena and thin film PbS.

No impurity peaks were observed in the bulk of the PbS film. AES scans of the surface of most of the PbS films show, in addition to the prominent Pb and S peaks, other Auger peaks at energies corresponding to Iron (47,598,651, 703 eV) and Chlorine (181 eV). This surface contamination may be caused by impurities present in the chemical solutions. For example, actual lot analysis performed by the manufacturer on the lead nitrate crystal used to form one of the chemical ingredients of the reaction shows the presence of both Cl and Fe at 0·001% each. On the film surface an oxygen peak (510 eV) is also present. This peak, however, soon disappears upon etching. To produce an Auger spectrum of a contamination-free PbS surface generally required the sputter etching of approximately the top 100Å. Several workers have reported [12, 13, 14] the presence of oxygen near the surface of PbS. Hence, it seems plausible to subscribe to the proposal [15] which suggests that the rapid decrease of the oxygen peak detected near the surface is due to excess concentration there rather than preferential sputtering of oxygen.

Changes in S:Pb ratio at the surface with respect to the bulk were used to detect changes in composition. On the other hand changes in the bulk S:Pb ratio from one sample to the other can not be explained. It may be partly due to changes in the surface roughness of the investigated areas [12]. Large changes in stoichiometry from one film to the other causing strongly degenerate conditions are ruled out since all PbS films exhibited strong and reproducible photovoltaic characteristics for photon energies equal to or larger than the band gap.

Results

Auger Profiles of the PbS-Si Heterostructure

The purpose of the experiments described in this section is to show that the PbS-Si samples prepared by the chemical deposition of PbS on Si result in a direct contact between the two semiconductors. The depth profile of a 2000Å PbS film grown on a Si (100) substrate, sample G5, is shown in Fig. 2. The elemental lines are plotted in arbitrary units

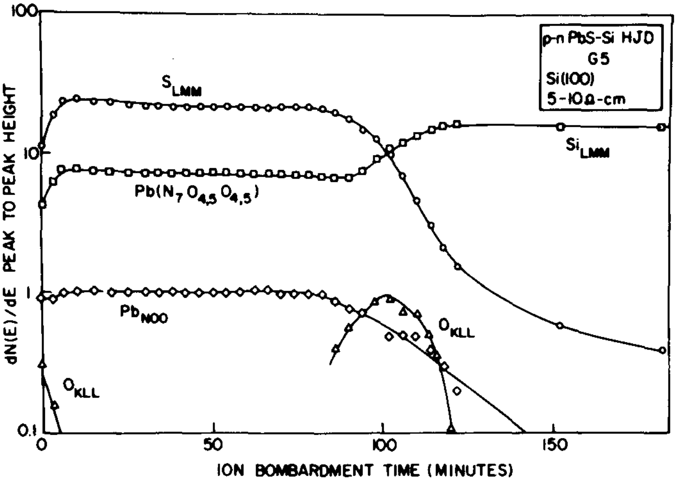

Fig. 2 AES Composition vs. Ion Bombardment Time

on a logarithmic scale varsus the ion bombardment time on a linear scale. The Si peak is first detected after 90 min. of ion bombardment.

The oxygen peak detected at the PbS-Si interface was about three times larger than that detected at the surface of the polycrystalline PbS film. However, this ratio was different from sample to sample and was dependent on the post deposition treatment. The planar distribution of surface constituents at the surface of the PbS film is shown in Fig. 3. The average variation of the S:Pb peak ratio lies within ± 1.5% over a 2mm distance, thus suggesting uniform surface composition. The oxygen surface concentration exhibited considerably more variation, with the S:O ratio varying ± 19% over a 2mm distance.

The surface composition of PbS films was studied. The relative intensities of the sulfur and lead lines, at 152 eV and 90 to 94 eV, were evaluated at several points on the surface. The average S:Pb peak ratio on the surface was calculated and compared to that computed by averaging the same ratio throughout the bulk. This average is tabulated

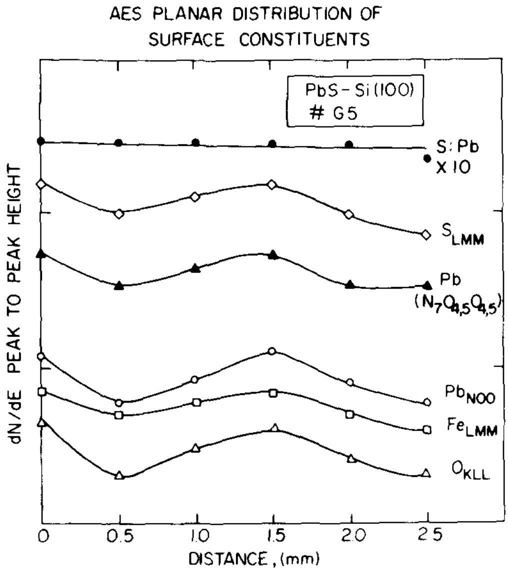

Fig. 3 AES Planar Distribution of Surface Constituents.

in Table III. The average is referred to as the $<S:Pb_1>$ ratio at the surface. The $<S:Pb_1>$ ratio was also calculated from the Auger scans of the first 150Å below the surface. The average of these calculations is also presented in Table III. It was found that the S:Pb ratio at the surface of the PbS film is smaller than that in the bulk. Differing sulfur and lead sputtering rates cause at least part of this S:Pb ratio surface variations. It seams also that the sulfur concentration at the surface is lowered drastically by long term, low temperature heat treatment in air, samples G_3 and G_6. Little effect is noted when the heat treatment is performed in N_2 environment, samples G_4 and G_7. Fig. 4 illustrates this effect, where the $<S:Pb_1>$ ratio is plotted vs. sputtering depth for samples G_3 and G_6 (heat treated in air environment), sample G_5 (no heat treatment) and G_4 (heat treated in N_2

SAMPLE NUMBER	SAMPLE CHARACTERISTICS		$<S:Pb_1>$ SURFACE RATIO	$<S:Pb_1>$ RATIO ON SURFACE LAYER[A]	$<S:Pb_1>$ BULK RATIO
G_2	Untreated		2.7	2.8	2.8
G_3	Air	PbS-Si (111)	0.4	1.5	2.8
G_4	N_2		2.3	2.7	2.9
G_5	Untreated		2.7	3.0	3.0
G_6	Air	PbS-Si (100)	0.5	1.9	3.0
G_7	N_2		2.8	3.2	3.0

(A) The average is computed over 300 A thick surface layer.

Table III Comparison between Surface and Bulk Composition environment). It is interesting to note that in all cases the <S:Pb$_1$> ratio converged to approximately the same steady state value in the bulk. The S:Pb$_1$ ratio at the surface of a thick PbS film (4000Å, sample VII) is greater than that in the bulk. This is the opposite of what was observed in the case of thin PbS films, as shown in Table III. This thick film sample was prepared by maintaining the Si substrate in the growth solution for 80 min.

The film thickness, as measured by the gravimetric method, is used to calculate the sputter etch rate and the sputter yield of PbS. For example the average PbS film thickness, by weight, for sample G1 (PbS-glass) is 2000Å ± 3%. The ion bombardment time required to reach the interface was 100 min. Hence the PbS sputter etch rate is 20Å/min. A (100) PbS film orientation is assumed on (100) Si substrates [17] resulting in 5.68×10^{14} Pb and S ions per cm^2. Using the 2 kev Ar ion parameters of 3 μA current and 1 cm beam diameter the sputter yield of PbS is calculated to be 5.5 atoms/ion.

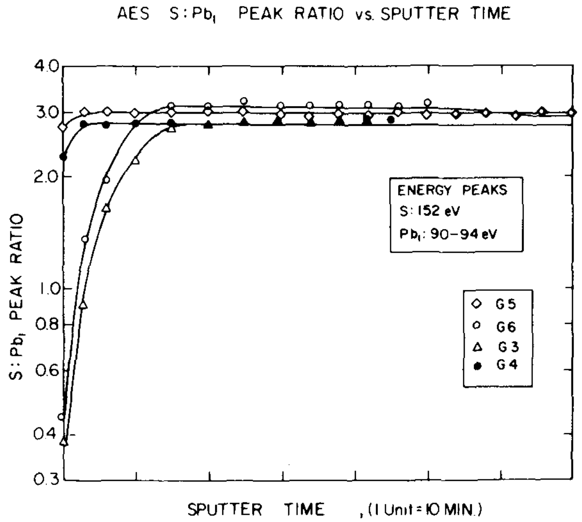

Fig. 4 AES S:Pb$_1$ Peak Ratio vs. Sputter Time.

Considerations of sputter yield and etch rate impact dramatically on the evaluation of the PbS-Si interface width. Fig. 5 demonstrates the Auger depth profiles of a PbS film grown on (100) Si substrate. The interface width of SiO$_2$-Si and AlGaAs-GaAs heterojunctions have been measured [18] from Auger depth profiles by extrapolating the steepest slopes of elemental profiles on both sides of the interface. This procedure is demonstrated in Fig. 5 An approximate value for the "real" interface width, ΔW, is obtained from [18]

$$\Delta W = \Delta W_M - \lambda - 2r \qquad (1)$$

where ΔW_M is the measured interface width, λ is the electron escape depth and r is the ion range.

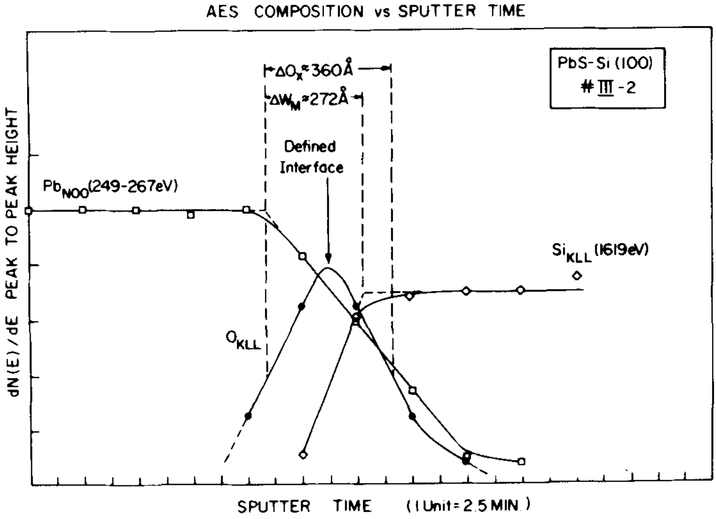

Fig. 5 Composition vs. Sputter Time, PbS-Si(100), #III-2

The interface parameters of wide and narrow beam Auger profiles are compared in Table IV for the wide and narrow beam Auger profile presented in Figs. 5 and 6. Since no r and λ values exist for PbS, we inserted the corresponding values for Si in Eq. (1). An alternative method to determine the interface width is to use the distance over which the Si line increases from 20% to 80% of bulk value. This parameter was calculated using the Si_{KLL} line and is also tabulated in Table IV along with the width of the oxygen peak at half maximum, ΔOx.

PARAMETER	Wide Beam Profile$^{(A)}$		Narrow Beam Profile$^{(B)}$	
	ΔW_M (Å)	ΔW(Å)	ΔW_M(Å)	ΔW(Å)
Si_{KLL} - Pb_{NOO}	272	216	225	191
Si_{LMM} - S_{LMM}	448	428	239	169
(0.2 - 0.8) Si_{KLL}	85		83	
ΔOx	360		72	

(A) Auger beam diameter = 0.05 - 0.08 cm. The Auger profile is presented in Fig. 4.

(B) Auger beam diameter = 10^{-4} cm. The Auger profile is presented in Fig. 5.

Table IV Interface Parameters of the PbS-Si HJ

The wide beam profiles of Figs. 2 and 5 were obtained using an Auger beam of 0.05 to 0.08 cm diameter. Hence the interface width evaluated from these profiles reflect to a significant degree the surface roughness of the PbS film. The narrow beam profile of Fig. 6 was obtained on a PHI-SAM 590 System using a 10^{-4} cm Auger beam and a rastered ion beam. The Auger beam was placed on the flat region of the PbS film away from any clusters. Hence the interface parameters evaluated in this case from Fig. 6 are substantially smaller than the corresponding parameters of Fig. 5, as can be seen from Table IV.

The Auger analysis of the PbS-Si interface has shown the major impurity to be oxygen with a concentration of 1 at.%. The chemical form of this oxygen is not known. The absorption and incorporation of oxygen by polycrystalline PbS has been shown [12] to occur at room temperature. Significant presence of silicon oxides is unlikely since etching of the Si substrate is conducted immediately prior to the PbS growth. The Si substrate is not exposed to air after etching but it is transferred from a water bath immediately to the PbS growth solution in N_2 environment.

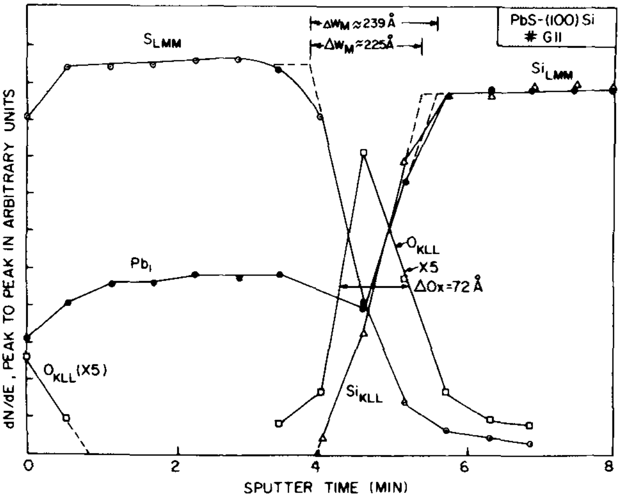

Fig. 6 AES Composition vs. Sputter Time
PbS-Si(100), #G11

The high solubility of SiO_2 in solution of NaOH has been reported [19] and this suggests that silicon oxides would disolve rather than form during the reaction. Judging from thermodynamic data, namely the heat of formation, PbO is far more likely to form than SiO_2. However, the x-ray diffraction pattern of PbO was not detected on these samples [2]. Consequently only minute amounts of PbO could be present at the interface and escape detection. The same is true for oxygen detected at the surface of the PbS films. Scanning electron microscope (SEM) surface studies [2] on these samples indicate the presence of PbS crystallites only, thus ruling out anything but a minute amount of PbO.

Auger Profiles of Multilayer PbS Films

The purpose of the experiments described in this section was to study the chemical structure of PbS-Si HJ formed by growing a multilayer PbS film on Si substrates. The growth of thick PbS films is desirable in order to increase the photovoltaic signal and hence improve the detectivity of the PbS-Si HJ. Since the maximum thickness of PbS films grown on Si substrates from a chemical growth solution is presently limited to about 6000Å, the growth of thicker PbS films is accomplished by sequentially growing PbS layers in several chemical baths. This multilayer PbS film is widely used in making photoconductive infrared detectors in industry.

The composition-depth profile of such a multilayer PbS film grown on a Si substrate (sample VI) is shown in Fig. 7 This sample is prepared by sequentially introducing the Si substrate into three identical PbS chemical growth solutions with 25 min. growth period allowed in each. The transfer between chemical solutions was performed without washing or drying the sample in between and with no exposure to air. The thickness of the three PbS films grown on the Si substrate was evaluated from the AES depth profiles, Fig. 7, by comparing the etch depth between the oxygen maximum at the PbS-PbS interfaces, to the total film thickness, 4500Å. The first PbS film grown on the Si substrate is 1900Å thick, the second and third films are 1500Å and 1100Å thick, respectively. No change in the magnitudes of the Pb and S peaks occurred between one film and the next. The P:S ratio remained constant throughout the three PbS films, which shows that no major change in composition occurs in the different layers. It is important to note the presence of an oxygen peak at the interface of each film as well as at the PbS-Si interface. The oxygen peak at the PbS-Si interface is 1.8 times larger than that present at the PbS-PbS interfaces. The relatively large accumulation of oxygen at the PbS-Si interface may be due to the misfit between the structure of the two materials resulting in a large density of Si dangling bonds, theoretically estimated to be ~ 1x $10^{15}/cm^2$. The presence of the oxygen peak at the interface region between consecutive PbS films is found to have no effect on the Pb:S Auger peak intensity ratio.

The planar spatial distribution of surface constituents at the PbS-PbS interface (sample VI) was also investigated. This data was obtained by recording the AES spectra at nine different positions, 1 mm apart, 1900Å below the surface of the final PbS film, where the maximum of the oxygen peak is detected between the first and second PbS films. The sample was etched with a defocussed Ar beam to avoid lateral nonuniformity of the sputter etch rate and all positions on the sample can be considered to be roughly at equal depth. The

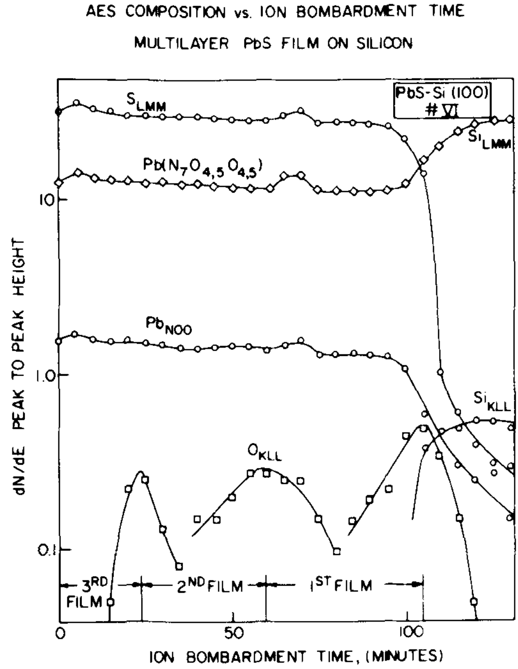

Fig 7 Multilayer PbS on Si(100)

S:Pb peak ratio was found to be constant at all inspected positions. The sulfur to oxygen ratio at the PbS-PbS interface was observed to vary ± 17% over this 2 mm distance, which is quite similar to the variation observed at the PbS surface.

Although multiple depositions of PbS film on Si yield a thick film with uniform composition, it is not known whether the presence of oxygen at the PbS-PbS interfaces may alter the carrier transport properties through the PbS-Si heterojunction. Although no contamination in the bulk of the PbS film was detected, the change in impurity concentration in the films may cause the formation of rectifying junctions at PbS-PbS interfaces.

Effect of Heat Treatment on Au-PbS Contact

Composition-depth profiles obtained with Auger electron spectroscopy and in situ sputter etching were used to observe the effect of low temperature ($T < 200°C$) treatment in air on the interface between evaporated gold layers and polycrystalline thin film PbS. This preliminary experimental study is similar to a previous study [20] that evaluated the interdiffusion occurring in the Au/GaAs, and Ni/Au-Ge/GaAs thin film system due to heat treatment ($T=250$ to 370°C). Evaporated gold films should provide ohmic contacts to p-type PbS layers and to p-n PbS-Si heterojunctions. Since the Au work function, 4.8 eV, is larger than that for PbS, 4.0 eV [21] the PbS is accumulated at the Au-PbS contact. Contact electrical stability and mechanical strength are necessary for the satisfactory operation of the heterojunction detector. It must be noted that as-deposited Au layers peel off PbS films easily and therefore bonding is generally very difficult. However, after heating in air at 100°C or 200°C for 3 hrs or more the Au contact to PbS has a far greater mechanical strength and ultrasonic bonding is greatly simplified.

Samples G_8 and G_9 were prepared to study the effect of low temperature heat treatment on the Au-PbS contact on a Si substrate. A Au film was evaporated over the surface of the PbS layers. In sample G_8 the gold film was thinned down by dipping in aqua regia in order to reduce the ion bombardment time required to reach the interface. In sample G_9 the Au

PbS-Si structure was heated at 200°C for 3 hours in air prior to thinning down the Au film in aqua regia.

A typical depth-composition profile for a Au/PbS-Si system, sample G_8, is shown in Fig. 8 The Auger spectra of the sample were recorded every four min. during sputter etching. The peak-to-peak amplitude of an Auger line of each constituent of the Au/PbS-Si System is plotted on the same vertical scale. The Au and O lines are magnified by a factor of 10 and 100 respectively. A substantial amount of oxygen, the O_{KLL} line at 510 eV, is observed at the Au-PbS interface. The contaminants are primarily associated with the Au layer and disappear after sputter etching. The thickness of the PbS film evaluated by the gravimetric method is 2000Å.

The oxygen peak at the Au-PbS interface is half that at the PbS-Si interface. The amplitude of the oxygen peak was compared to that in SiO_2 spectra to estimate the atomic percentage oxygen present at the surface and interface. The comparison yield 0.7 and 1.5% for surface and interface concentration, respectively.

The effect of heat treatment on the chemical profile of the Au/PbS-Si structure can be seen in Fig. 9, where G_8 is the as-deposited sample while G_9 underwent heat treatment in air at 200°C for 3 hrs. For the heat treated sample, G_9, the total amount of Au accumulating near the surface has increased and the Au-PbS interface moved deeper into the PbS film. The maximum oxygen peak is observed ~ 860Å deeper than in the untreated sample. Before an accurate interpretation of the data shown on Fig. 9 can be made, the influence of ion bombardment on the profile of the Au/PbS-Si structure must be known. Since the observed composition of the metallic film varies differently with depth for samples G_8 and G_9, the sputter yields of the Au, Pb, S and O would be expected to vary with depth. Thus the depth scale of Fig. 9 should probably be corrected to take into account the varying sputter yields. Quantitative corrections for these bombardment effects in the Au/PbS-Si system are not yet established. Hence, in Figs. 8 and 9 the assumption of equal Au and PbS sputter etch rates is used. This assumption is not unreasonable since the sputter yield of Au at 2 keV Ar ion energy is roughly 4.2 atoms/ion [22] whereas that calculated for PbS is 5.2 atoms/ion, or only 25% higher.

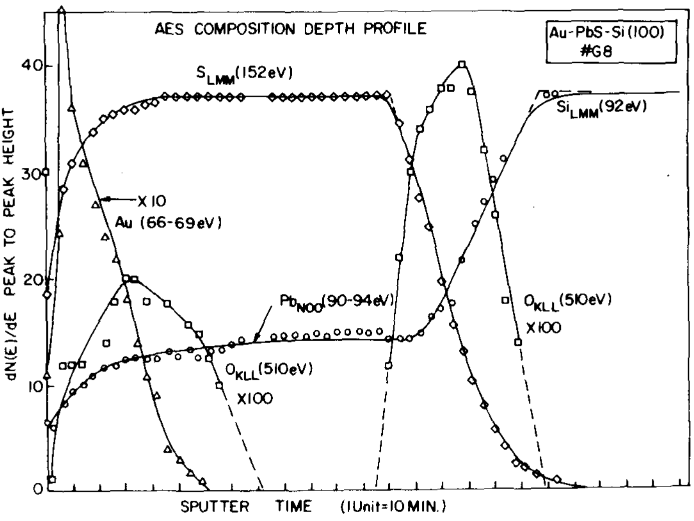

Fig. 8 AES Composition vs. Sputter Time
Au-PbS-Si

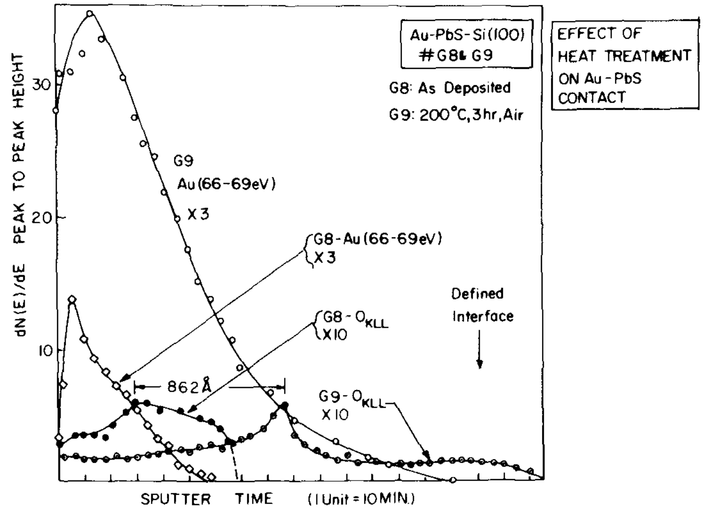

Fig. 9 Effect of Heat Treatment (200°C, 3hr, Air)
on Au-PbS Contact

The area under the profile of the Au peak of Sample G_9 is 7 times larger than that for sample G_8, as shown in Fig. 9. Heat treatment thus results in increasing the population of Au atoms in the thin PbS films. The deeper oxygen profile observed in the treated sample G_9 suggests that the oxygen travels along with the gold into the PbS film.

Discussion and Summary

The effect of low temperature heat treatment on the composition of polycrystalline PbS films and PbS-Si heterostructures was also examined and is discussed in this section. The object was to determine any possible effects the PbS chemical structure might experience during the bake-out period used for PbS and PbS-Si HJ detectors. The heat treatment consisted of 24 hrs at 100°C in air or nitrogen ambients. The effect of heat treatment on the oxygen peak present at the PbS film surface and PbS-Si interface is shown as the sulfur to oxygen peak ratio in Table V. While exact quantitative conclusions are difficult to obtain from the variations of the <S:O> ratio for various samples, a number of qualitative statements can be made. The effect of heat treatment in air definitely increases the oxygen concentration both at the PbS film surface and the PbS-Si interface for (100) as well as (111) Si substrates. The effect of heat treatment in N_2 ambient was also to increase the oxygen concentration at the interface. While one can safely ascribe the increase in oxygen surface concentration during air heat treatment to oxidation, it is not clear what happens at the PbS-Si interface. Apparently the interface acts as a getter for impurities like oxygen, and heat treatment enhances the accumulation of oxygen.

The S:O ratio at the PbS-(111) Si interface was twice that found at the PbS-(100) Si interface. The change in the oxygen peak height with substrate orientation suggests that more oxygen bonds are present at the PbS-(100) Si interface than at the PbS-(111) Si interface [17]. This is consistent with the higher density of dangling bonds present on the (100) Si surface as compared to the (111) Si surface but contrary to what is expected from measurements performed on bare Si surfaces. These measurements show that the O:Si ratio at the surface of (111) substrates is higher than in (100) substrates.

SAMPLE		$Pb_1:O^{(C)}$	$S:O^{(A)}$	
NUMBER	CHARACTERISTICS	SURFACE$^{(B)}$	SURFACE$^{(B)}$	INTERFACE
G_2	Untreated	24	69	19
	PbS-Si (111)			
G_3	Air	17	16	4
G_5	Untreated	33	100	10
	PbS-Si (100)			
G_6	Air	9	12	3

(A) S_{LMM} (152 eV):O_{KLL} (510 eV)

(B) Approximately 30Å below surface.

(C) Pb_{NOO} (90-94eV):O_{KLL} (510 eV)

Table V Oxygen Content at the PbS Film Surface and at the Interface of PbS-Si HJ

It is interesting to point out that the resistivity of PbS films has also been observed to increase with heat treatment in air. The sheet resistance of PbS films was measured by the four probe method. These measurements yield an equivalent bulk dark resistivity in the 5 to 10 ohm-cm range. PbS films annealed for a few hours at temperatures between 100°C and 200°C, exhibited bulk resistivity increases of an order of magnitude. Fig. 10 shows the variation in the resistivity versus anneal period, at 150°C, for PbS films grown on glass substrates. A preliminary explanation for this experimental data is that increased oxygen absorption in the surface layer of the PbS film produces an increase in the film resistance. The change in resistance is large and

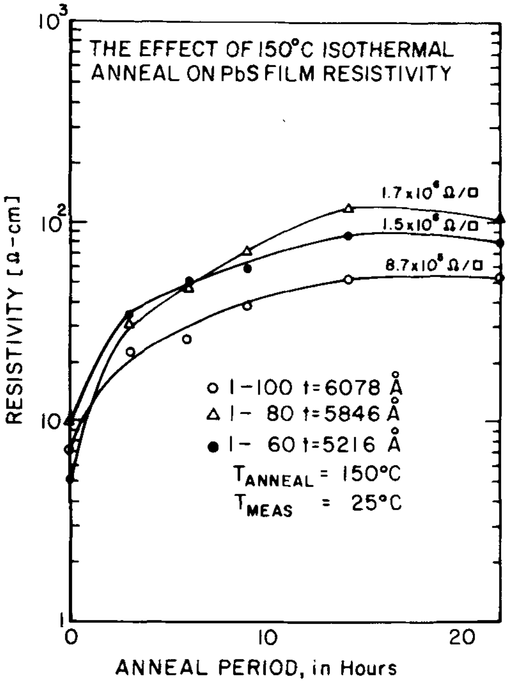

Fig. 10 The Effect of 150°C Isothermal Anneal on PbS Film Resistivity

detectable for films that are 0.5 μm thick. These results are in agreement with previous experimental work [12]. Thermoelectric type measurement, by hot probe method, carried out on these PbS films grown on glass substrates reveal that they display p-type conductivity.

The present work confirms the results obtained by others [12, 13, 14] that extensive oxygen adsorption occurs in PbS films. The exact chemical state of this oxygen presence is unknown. However, since the oxygen presence at the surface is paralleled by sulfur deficiency for the heat treated samples, this may suggest the presence of a thin lead oxide layer at the surface. Lead oxides do not form separate crystallites in this case [2], but must be dispersed on the surface of the PbS crystallites. This in turn can represent layers of high resistance which would increase the film resistance.

Heating the growth solution to 80°C enhances the reaction and deposition rates without altering the profiles of the different elements. It also increases the sulfur to oxygen ratio at the surface and interface. The oxygen content at the PbS-Si interface of HJs formed on unpolished (100) Si substrates is substantially higher than that observed on polished substrates.

A complete quantitative interpretation of the PbS Auger spectra in terms of the concentrations of individual constituents would require knowledge of the ejection depths of the Auger electrons, that is data on the mean free path of the primary and Auger electrons. Also, knowledge of the capture cross section of the Auger process for Pb and S as well as their varying sputter yields is required. However, a theoretical treatment and experimental data for handling the PbS-Si Auger trace are not yet available. Thus, only qualitative estimates of surface compositions have been made using Auger line intensities.

In conclusion, the formation of PbS-Si heterojunctions by chemical deposition of PbS on a Si substrate at room temperature was verified by Auger analysis of the PbS-Si interface. The oxygen line is the only major impurity (~ 1% atomic concentration) detected at PbS-Si interface, at interfaces between successive PbS films as well as at the top film surface.

Acknowledgments

The authors wish to thank Professor J. B. Hudson and K. Malony for their assistance with the Auger spectroscopy of the samples and many helpful discussions. Discussions with Dr. P. Lindfors of Physical Electronics Industries Inc. on sputter yield and etch rate calibration are also gratefully acknowledged.

References

[1] H. Elabd and A. J. Steckl, J. Vac. Sci. Tech. 15, 264 (1978).

[2] H. Elabd and A. J. Steckl, J. Appl. Phys. 51, (1980).

[3] A. J. Steckl, H. Elabd and T. Jakobus, Tech. Digest IEDM, IEEE Cat. No. 77 CH 12757ED, 549, (1977).

[4] A. J. Steckl, M. E. Motamedi and S. P. Sheu, Proc. IRIS, 132900-4-x, 401, (1978).

[5] A. J. Steckl, M. E. Motamedi, S. P. Sheu, H. Elabd and K. Y. Tam, Proc. CCD '78 Conference, 239, San Diego, CA (1978).

[6] P. Auger, Surface Science 48, 1 (1975).

[7] R. W. Weber and A. L. Johnson, J. Appl. Phys. 38, 4355 (1967).

[8] J. H. Richardson and R. V. Peterson, Systematic Materials Analysis, Academic Press, N.Y. (1974).

[9] C. Chuan Chang, Surface Science 25, 53 (1971).

[10] P. R. Norton, R. L. Tapping and J. W. Goodale, Surface Science 65, 13 (1977).

[11] Paul W. Palmberg, et al. Handbook of Auger Electron Spectroscopy, Physical Electronics Industries Inc., Edina, Minnesota (1972), and Information from The Analytical Lab. of Physical Electronics Industries, Inc.

[12] L. J. Hillenbrand, J. Chem. Phys. 41, 3971 (1964), and L. J. Hillenbrand, J. Phys. Chem. 73, 2902 (1969).

[13] R. N. Lee, J. de Phys. 29, C4-43 (1968).

[14] Yu A. Zarif'yants and V. V. Kuryler., Sov. Phys. Semicond. 7, 3, 414 (1973).

[15] M. S. Said and J. N. Zemel, J. Appl. Phys. 47, 3, 866 (1976).

[16] P. H. Holloway, Physical Electronics Industries, Inc. (unpublished).

[17] H. Elabd, A. J. Steckl, W. Vidinski, Presented to the Photovoltaic Material and Device Workshop, Arlington, VA. (1979) and H. Elabd, A. J. Steckl, W. Vidinski Solar Cells, 2, (1979).

[18] J. S. Johannessen, W. E. Spicer and Y. E. Strausser, J. Appl. Phys. 47, 7, 3028 (1976); C. R. Helms, W. E. Spicer and N. M. Johnson, Solid State Commun. 25, 673 (1978); and C. M. Garner, C. Y. Su, W. E. Spicer, P. D. Edward, D. Miller, and J. S. Harris, Appl. Phys. Lett. 34, 610 (1979).

[19] I. M. Kolthoff and P. J. Elving, Treatise on Analytical Chem. Part II, 2, 121., Sect. A. (1962).

[20] G. Y. Robinson, J. Vac. Sci. Tech. 13, 884 (1976).

[21] T. Grandke and M. Cardona (unpublished).

[22] J. M. Poate, K. N. Tu, and J. W. Mayer. Thin Films Interdiffusion and Reactions", John Wiley Inc. (1978).